

Application of Subject Specific Models for Mapping Brain Function with Diffuse Optical Tomography

Yuxuan Zhan¹, Hamid Dehghani¹, Brian R. White² and Joseph P. Culver²

¹ School of Computer Science, University of Birmingham, United Kingdom

² Department of Radiology, Washington University, St. Louis, MO 63110, USA
yx:986@cs.bham.ac.uk

Abstract: The application of diffuse optical tomography (DOT) methods for neuroimaging of humans is challenging due to the geometry of each individual subject and light level constraints. A high density imaging array system has been developed and used to demonstrate the possibility of true tomographic reconstruction of cortical activity within the adult subjects which are consistent with studies using functional MRI and positron-emission tomography. This work demonstrates the benefits of using subject specific models for image reconstruction and investigates depth related information available from the increased number of tomographic measurements.

©2010 Optical Society of America

OCIS codes: 110.6955 (Tomographic imaging), 100.6950 (Tomographic image processing), 170.2655 (Functional monitoring and imaging), 170.3660 (Light propagation in tissues)

1. Introduction

Noninvasive optical imaging techniques have led to large advancements in neuroscience, allowing the functional mapping of the human brain on a scale that is only accessible through invasive studies of animals [1]. A promising potential for clinical neuroimaging has emerged to provide longitudinal diagnostic and prognostic studies about brain function. The majority of research studies in healthy adults are conducted with functional magnetic resonance imaging (fMRI), which due to its high cost, fixed scanner locations, and inability to comprehensively assess altered brain metabolism is essentially limited to its translation as a bedside clinical tool. Diffuse optical tomography (DOT) is a novel and non-invasive imaging methodology that is uniquely suited to this setting, as it is a mobile system utilizing a small, flexible imaging cap [2] and can measure absolute changes in oxygenated (ΔHbO_2), deoxygenated (ΔHbR), and total hemoglobin (ΔHbT), providing more comprehensive images of the brain's hemodynamics.

DOT provides a large variety of technological improvements to resolution and depth-sectioning including the use of high-density arrays of optodes (near infrared sources and detectors). In a recent study, a new high-density DOT system with high contrast-to-noise was presented and the ability to image brain responses in adult humans with greater detail than was previously accessible to optical imaging was demonstrated [3]. These advances in image quality were made possible through increased dynamic range, allowing the inclusion of light from multiple source-detector separations in the image reconstructions.

As this demonstration of the promise of DOT was confined to a small lateral region of brain and only to the superficial cortex, a relatively simple model of light propagation for image reconstruction was sufficient. The head was assumed to be a hemisphere (8 cm radius) and consisted of only two layers (scalp/skull and brain). Many other optical studies use still simpler imaging strategies including semi-infinite models to estimate the sensitivity of different source-detector pair measurements [4, 5]. However, as future DOT systems will cover larger regions of the head, taking into account the true contour of the head and perhaps internal layers, will be crucial to accurate localization of brain activity [6]. In addition, continuous sampling of the cortical grey matter will require sensitivity and depth localization of changes deep into the sulcal folds.

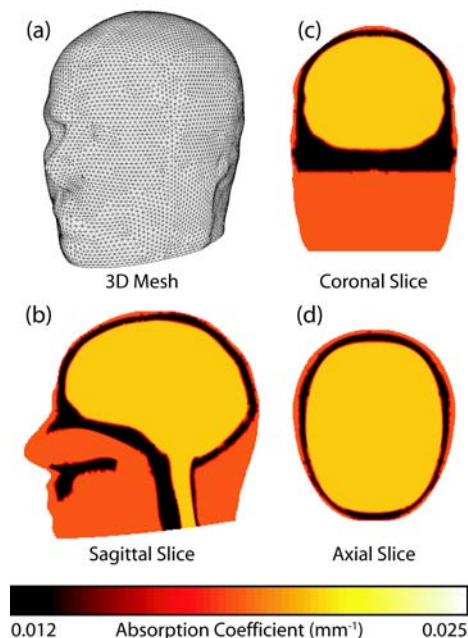


Figure 1. Three dimensional (3D) model of the adult brain. (a) View of the FEM mesh. (b-d) Cross-sectional maps of absorption at 849 nm.

In this work, we present numerical simulations using a finite element model (FEM) of the adult head to study the image quality as a function of the imaging model as well as array and data sampling strategy for high-density DOT systems.

2. Methods

The numerical model used is a three-dimensional (3D) FEM representation of the adult head, Figure 1(a). The underlying geometry was created through the combination of manual segmentation of an MRI dataset and other anatomical reference models using a commercial surface modeling tool. The mesh contains 88,492 nodes corresponding to 502,526 linear tetrahedral elements. Three different regions were considered: muscle/skin, bone, and brain. We used the physiological and optical parameters for different regions as determined in Torricelli et al. [7]. The optode array was placed over the occipital cortex of the anatomic model (Figure 2). Using NIRFAST

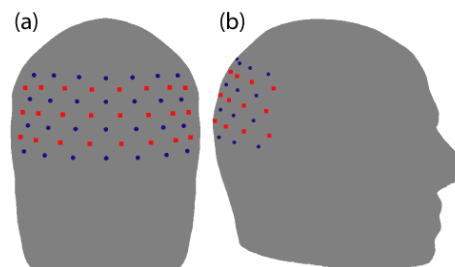


Figure 2. (a) Back view and (b) side view schematic showing the placement of the imaging grid over the visual cortex of the adult head model with 24 sources (red squares) and 28 detectors (blue circles).

	1 NN	2 NN	3 NN	4 NN	5 NN
Number of measurements included	84	212	260	348	396
Maximum source/detector separation (mm)	13	30	40	48	54

Table 1. The total number for measurements for 24 sources and 28 detectors using either 1st, 2nd, 3rd, 4th, or 5th nearest neighbor (NN) combinations.

[8], light propagation within the head model was simulated for all five combinations. The details of the number of measurements and the maximum distance of source detector pairs for each of these detection strategies are shown in Table 1.

Test images of focal activity at different depths were evaluated. Simulated reference data was generated using the unperturbed model shown in Figure 1. Brain activation were modeled at varying depths using a small (0.5 cm radius) hemodynamic change consisting of a 3.8 μM rise in total hemoglobin and 3.76% change in oxygen saturation (final anomaly values of $\text{HbT} = 79.8 \mu\text{M}$, $\text{SO}_2 = 74.76\%$ against background brain values). Differential intensity data was calculated based on changes at 849 nm. Consistent with current *in vivo* performance, 0.15% random noise was added to both the reference (unperturbed) and anomaly (perturbed) data. The noise added was calculated as a set of randomly distributed Gaussian noise, at each data point and dataset. Assuming no knowledge of the background optical properties of the volume being imaged, the noise-added unperturbed data was used to calculate a global fit for background (unperturbed) absorption. Assuming a background reduced scattering coefficient of 1.0 mm^{-1} , the calculated global value for the absorption coefficient, using this method was found to be $8.7 \times 10^{-3} \text{ mm}^{-1}$. Using a Jacobian based on these global optical properties, images of baseline (temporal change) activity were reconstructed using the difference data (perturbed – unperturbed).

3. Results

In order to highlight the differences in increased sensitivity and depth recovery between the different data sampling strategies, images of temporal changes due to small focal hemodynamic changes were reconstructed (Figure 3). The 1 NN measurement strategy is unable to reconstruct activations at any depth within the brain. Increasing the number of measurements used in the reconstruction from 2 NN to 5 NN increases the distance into the brain at which activations can be reconstructed. The 2 NN strategy is sufficient to image brain activity near the surface of the brain (corresponding to cortical gyri),

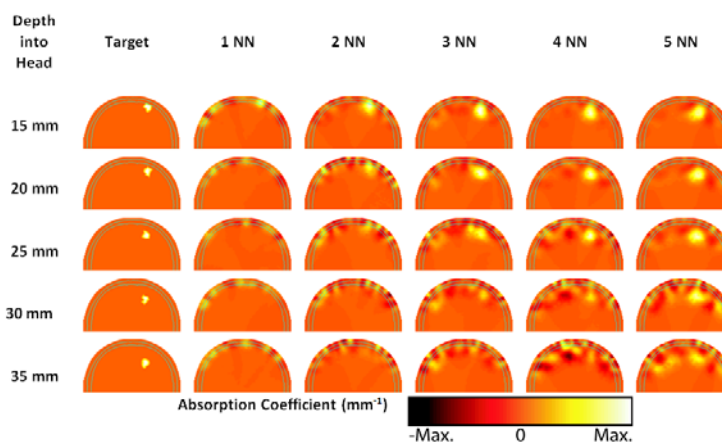


Figure 3. Reconstructed baseline tomographic images of hemodynamic activation at different depths within the brain. Only the back portion of the axial view of the 3D adult head model is shown, with solid cyan lines representing the skull outline.

while the 5 NN strategy can image to at least 20 mm deep within the brain, which allows measurement of activity within sulcal folds.

4. Conclusions

Images of small baseline hemodynamic changes were reconstructed using noise added simulated data and a model of “calculated bulk” optical properties. From the reconstructed images, it is clearly seen that although the 2 NN data sampling can recover a modest change at 5 mm deep within the brain, the ability to recover changes deteriorates dramatically for deeper regions. However, using 5 NN, changes at up to 20 mm deep within the brain are successfully recovered, despite some small reconstruction artifacts. The results presented give an indication of the future of in vivo DOT reconstructions and provide a roadmap for how to obtain the desired sensitivity throughout the cortical folds. Our modeling predicts a dramatic increase in depth sensitivity attainable using the 5th nearest neighbor measurements. Forward model sensitivities, inverse problem updates, and simulated image reconstructions show that such a system would be able to image at depths of or greater than 20 mm within the brain. Such sensitivity would allow the measurement activations at the bottom of sulcal folds. These results motivate future technological developments and will serve as a basis for accurate in vivo image reconstructions.

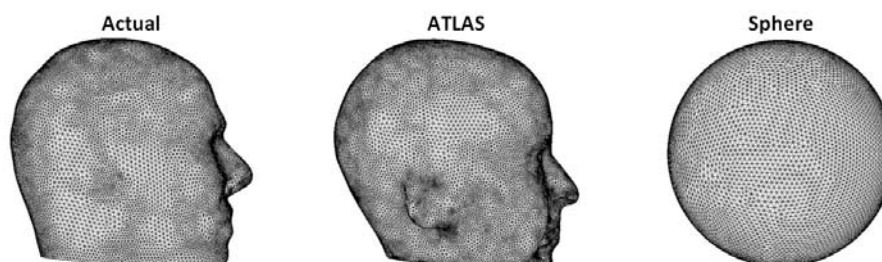


Figure 4. Examples of subject specific, generic ATLAS or simplified Spherical models.

The results presented have demonstrated that the use of subject specific models in accurate recovery of brain activation. In the future development, we will investigate the use of subject specific models as compared to the use of simplified or generic ATLAS models, as demonstrated in Figure 4. Generic models can be modified to match the subject specific external features using well established affine transforms and should in principle provide more accurate results as compared to simple models such as spheres. Additionally, the advantage of the use of generic models allows the elimination of structural imaging acquisition, such as MRI where not accessible. Nonetheless, results will be presented that will evaluate the accuracy of these generic models.

5. Acknowledgements

This work was supported by National Institutes of Health Grants K25-NS4339, R21-EB7924 and R01EB009233.

6. References

1. Strangman, G., Boas, D. A., Sutton, J. P., *Non-invasive neuroimaging using near-infrared light*. Biological Psychiatry, 2002. **52**(7): p. 679-693.
2. Obrig, H., and Villringer, A., *Beyond the Visible—Imaging the Human Brain With Light*. Journal of Cerebral Blood Flow & Metabolism, 2003. **23**: p. 1–18.
3. Zeff, B.W., et al., *Retinotopic mapping of adult human visual cortex with high-density diffuse optical tomography*. Proc Natl Acad Sci U S A, 2007. **104**(29): p. 12169-74.
4. Selb, J., Stott, J. J., Franceschini, M. A., Sorensen, A. G., and Boas, D. A., *Improved sensitivity to cerebral hemodynamics during brain activation with a time-gated optical system: analytical model and experimental validation*. JBO, 2005. **10**: p. 011013
5. Patterson, M.S., C. B., and B.C. Wilson, *Time resolved reflectance and transmittance for the non-invasive measurement of tissue optical properties*. Appl. Opt., 1989. **28**: p. 2331-2336.
6. Gibson, A., Riley, J., Schweiger, M., Hebden, J. c., Arridge, S. R., and Delpy, D. T., *A method for generating patient specific finite element meshes for head modelling*. Phys. Med. Biol., 2003. **48**: p. 481-495.
7. Torricelli, A., Pifferi, A., Taroni, A., Giambattistelli, E. and Cubeddu, R., *In vivo optical characterization of human tissues from 610 to 1010 nm by time-resolved reflectance spectroscopy*. Physics in Medicine and Biology, 2001. **46**: p. 2227–2237.
8. Dehghani, H., et al., *Near Infrared Optical Tomography using NIRFAST: Algorithms for Numerical Model and Image Reconstruction Algorithms*. Communications in Numerical Methods in Engineering, 2008.